Research Paper
Computational Methods for Differential Equations
http://cmde.tabrizu.ac.ir
Vol. *, No. *, *, pp. 1-16
DOI:10.22034/cmde.2022.51967.2171

A numerical method for KdV equation using rational radial basis functions

Mansour Shiralizadeh[1,*], **Amjad Alipanah**[2], **and Maryam Mohammadi**[3]

[1] Department of Mathematics, Payame Noor University (PNU), Tehran, Iran.

[2]Department of Applied Mathematics, University of Kurdistan, Sanandaj, Iran.

[3] Faculty of Mathematical Sciences and Computer, Kharazmi University, Tehran, Iran.

Abstract

In this paper, we use the rational radial basis functions (RRBFs) method to solve the Korteweg-de Vries (KdV) equation, particularly when the equation has a solution with steep front or sharp gradients. We approximate the spatial derivatives by RRBFs method then we apply an explicit fourth-order Runge-Kutta method to advance the resulting semi-discrete system in time. Numerical examples show that the presented scheme preserves the conservation laws and the results obtained from this method are in good agreement with analytical solutions.

Keywords. KdV equation, RBF, rational radial basis function method, Runge-Kutta method.
2010 Mathematics Subject Classification. 65N99, 65N35, 74G15, 97N40, 65M50, 65D25.

1. Introduction

In this paper, we examine the third-order nonlinear KdV equation as follows

$$w_t + \varepsilon w w_x + \mu w_{xxx} = 0, \qquad x \in [a,b], \qquad t \in [0,T], \tag{1.1}$$

with the initial condition

$$w(x,0) = g(x), \qquad x \in [a,b], \tag{1.2}$$

and Dirichlet boundary conditions as

$$w(a,t) = h(t), \quad w(b,t) = l(t), \qquad t \in [0,T], \tag{1.3}$$

where μ and ε are positive parameters, and $g(x)$, $h(t)$ and $i(t)$ are known functions, the term $\varepsilon w w_x$ is the nonlinear term which makes wave steep and the term μw_{xxx} is the dispersion term describes the spreading of the wave.

The KdV equation plays a significant role in describing physical phenomena such as shallow water waves [20], bubble-liquid mixtures [31], waves in plasma physics [12, 33], conduit waves and magma flow. For more description see [4, 5, 17] and references therein. The KdV equation was initially given in 1895 by Korteweg-de Vries [20] and the exact solutions to some special cases have been presented in [11, 23, 35]. However, finding an analytical solution of the KdV equation is only possible for limited conditions, also there are many KdV equations that can not be solved analytically and hence the numerical solutions to study the KdV equation are very useful, many numerical schemes have been used to solve the KdV equation such as finite difference [13, 32], finite element [1, 18], Galerkin method

Received: 06 June 2022 ; Accepted: 30 October 2022.
∗ Corresponding author. Email: m.shiralizadeh@pnu.ac.ir .

[14], Haar wavelet method [26], differential quadrature method [2, 3, 27], RBF method [6, 7], adaptive RBF method [24], sinc collocation method [19], finite difference and collocation methods based on the B-spline functions [21], etc.

A specific feature of the KdV equation is that its solutions may show solitary waves, known as solitons, that maintain their original shape, velocity, and size after interactions. We must point out that numerical schemes that maintain some of the conserved values of the given differential equations may have more accurate behavior in time than those that do not preserve [9].

Since the KdV equation is an integrable Hamiltonian system, it has a large number of independent conserved quantities. To demonstrate the efficiency of the proposed method, we will examine three famous conserved values of the KdV equation in some numerical examples.

In recent years researchers have used meshless techniques to avoid the mesh generation. A meshless method, use a set of scattered points instead of meshing the domain of the problem. For more description see [10, 15, 22, 25, 29, 34] and references therein. The RBF methods are substantial instruments for scattered points interpolation and solving partial differential equations (PDEs). The collocation scheme is the base of methods such as RBF that use meshless procedure to find the numerical solution of PDEs.

When the underlying function or the solution of PDE is sufficiently smooth, RBF methods can produce exponential accuracy, but if the underlying function or the solution of PDE has steep gradients or discontinuities, the RBF method may produce solutions with oscillation. In such situations, the rational radial basis functions (RRBFs) method can be used to approximate derivatives of functions and to solve PDEs [28]. RRBFs method approximating solutions in nonlinear spaces generated by RBFs, are more computational expensive than the standard RBFs methods. For smooth problems the accuracy obtained from these methods may not be worth the additional computations. However, for problems with discontinuities and steep fronts these methods will be considerably more accurate and the additional computations will be justified.

Jakobsson et al. [16] used a RRBF method to interpolate functions with steep gradients. Sarra and Bai [28] extended the method of Jakobsson et al. to interpolate discontinuous functions and to solve Burger's equation. In [8] De Marchi et al. presented RRBFs-based partition of unity interpolation, and in [30] authors used the RRBFs method for solving the Sine-Gordon equation.

In this paper, we apply the RRBFs method for solving the Eq (1.1) with conditions given in the Eqs. (1.2)-(1.3), particularly when the equation has a solution with steep front or sharp gradients. However, solving the problem with RRBFs interpolation, to our knowledge, is new.

This paper is organized as follows: In Section 2, we introduce the RBF s and RRBFs methods. The method implementation is given in section 3. We analyze stability issues in Section 4. In Section 5 we present the results of numerical examples. Section 6 is dedicated to conclusion.

2. RBF s interpolation and Rational RBF s interpolation

2.1. **RBF s interpolation.** Let $\Gamma \subseteq \mathbb{R}^m$ be a bounded set, $X = \{\boldsymbol{x}_1^c, ..., \boldsymbol{x}_N^c\} \subseteq \Gamma$ a set of N distinct points, hereinafter referred to as centers, and $F = \{f(\boldsymbol{x}_1^c), ..., f(\boldsymbol{x}_N^c)\}$ a set of function values. A RBF

$$\psi(\boldsymbol{x}) = \psi\left(\|\boldsymbol{x} - \boldsymbol{x}^c\|_2\,,\, \epsilon\right), \qquad \boldsymbol{x}, \boldsymbol{x}^c \in \mathbb{R}^m$$

is a function of one variable $r = \|\boldsymbol{x} - \boldsymbol{x}^c\|_2$ that is centered at $\boldsymbol{x}^c$, which ϵ is a free parameter and is called the shape parameter [10, 28], also in this paper $m = 1$.

We use the following RBFs

$$\text{Inverse quadratic (IQ)} \qquad \psi(r) = \frac{1}{1 + (\epsilon r)^2},$$

and

$$\text{Gaussian (GA)} \qquad \psi(r) = e^{-(\epsilon r)^2},$$

as representative members of the class of strictly positive definite, global, infinitely differentiable RBFs in the examples.

A RBF interpolant is of the form

$$p(\boldsymbol{x}) = \sum_{k=1}^{N} c_k \ \psi\left(\|\boldsymbol{x} - \boldsymbol{x}_k^c\|_2 \, , \, \epsilon\right) \tag{2.1}$$

which the coefficients c_k are obtained by solving the linear system

$$A\mathbf{c} = \mathbf{f},$$

based on the interpolation conditions $p\left(\boldsymbol{x}_j^c\right) = f_j$ where $\mathbf{f} = [f(\boldsymbol{x}_1^c), ..., f(\boldsymbol{x}_N^c)]^T$. The elements of the matrix A are of the form

$$a_{jk} = \psi\left(\|\boldsymbol{x}_j^c - \boldsymbol{x}_k^c\|_2 \, , \, \epsilon\right), \qquad j,k = 1, ..., N. \tag{2.2}$$

A is a symmetric positive definite matrix and thus invertible. The evaluation of the interpolant (2.1) at M points $\boldsymbol{x}_k$ is done by multiplying $\mathbf{c}$ by E where the elements of the matrix E are of the form

$$e_{jk} = \psi\left(\|\boldsymbol{x}_j - \boldsymbol{x}_k^c\|_2 \, , \, \epsilon\right), \qquad j = 1, ..., M, \quad k = 1, 2, ..., N. \tag{2.3}$$

The first, second and third derivatives of RBF interpolant are of the form

$$D(p(\boldsymbol{x})) = \sum_{k=1}^{N} c_k \ D\left(\psi\left(\|\boldsymbol{x} - \boldsymbol{x}_k^c\|_2 \, , \, \epsilon\right)\right),$$

thus

$$D(p(\boldsymbol{x}_j^c)) = \sum_{k=1}^{N} c_k \ D\psi\left(\|\boldsymbol{x}_j^c - \boldsymbol{x}_k^c\|_2 \, , \, \epsilon\right),$$

therefore

$$D\mathbf{f} \simeq D\mathbf{p} = E_D\mathbf{c},$$

where $\mathbf{p} = [p(\boldsymbol{x}_1^c), ..., p(\boldsymbol{x}_N^c)]^T$ and the elements of E_D are of the form

$$(E_D)_{jk} = D\psi\left(\|\boldsymbol{x}_j^c - \boldsymbol{x}_k^c\|_2 \, , \, \epsilon\right), \qquad j,k = 1, ..., N.$$

and

$$D(D(p(\boldsymbol{x}))) = \sum_{k=1}^{N} c_k \ D\left(D\psi\left(\|\boldsymbol{x} - \boldsymbol{x}_k^c\|_2 \, , \, \epsilon\right)\right),$$

thus

$$D(D(p(\boldsymbol{x}_j^c))) = \sum_{k=1}^{N} c_k \ D\left(D\psi\left(\|\boldsymbol{x}_j^c - \boldsymbol{x}_k^c\|_2 \, , \, \epsilon\right)\right),$$

therefore

$$D(D\mathbf{f}\,) \simeq D(D\mathbf{p}) = E_{DD}\mathbf{c},$$

where the elements of E_{DD} are of the form

$$(E_{DD})_{jk} = D\left(D\psi\left(\|\boldsymbol{x}_j^c - \boldsymbol{x}_k^c\|_2 \, , \, \epsilon\right)\right), \qquad j,k = 1, ..., N.$$

and

$$D(D(D(p(\boldsymbol{x})))) = \sum_{k=1}^{N} c_k \ D\left(D\left(D\psi\left(\|\boldsymbol{x} - \boldsymbol{x}_k^c\|_2 \, , \, \epsilon\right)\right)\right),$$

thus

$$D(D(D(p(\boldsymbol{x}_j^c)))) = \sum_{k=1}^{N} c_k \ D\left(D\left(D\psi\left(\|\boldsymbol{x}_j^c - \boldsymbol{x}_k^c\|_2 \, , \, \epsilon\right)\right)\right),$$

therefore

$$D(D(D\mathbf{f}\,)) \simeq D(D(D\mathbf{p}\,)) = E_{DDD}\mathbf{c},$$

where the elements of E_{DDD} are of the form

$$(E_{DDD})_{jk} = D\left(D\left(D\psi\left(\|\boldsymbol{x}_j^c - \boldsymbol{x}_k^c\|_2\,,\,\epsilon\right)\right)\right), \qquad j,k = 1,...,N.$$

In the following theorem [8] we give an error bound in terms of the power function $P_{\psi,X}$, where $\mathcal{N}_\psi(\Gamma)$ is the native reproducing kernel Hilbert space corresponding to the symmetric positive definite RBF [10].

Theorem 2.1. *Let $\psi \in C(\Gamma \times \Gamma)$ be a strictly positive definite RBF, and suppose that $X = \{\boldsymbol{x}_1^c, ..., \boldsymbol{x}_N^c\} \subseteq \Gamma$ is a set of distinct points and p is the interpolant to $f \in \mathcal{N}_\psi(\Gamma)$. Then for all $\boldsymbol{x} \in \Gamma$ we have*

$$|f(\boldsymbol{x}) - p(\boldsymbol{x})| \leq P_{\psi,X}(\boldsymbol{x})\|f\|_{\mathcal{N}_{\psi(\Gamma)}}.$$

2.2. **Rational RBF interpolation.** The RBF interpolants have problems such as ill-conditioning especially when the shape parameter tends to zero and these problems might lead to inaccurate solutions particularly when the functions with steep front or sharp gradients are considered. Moreover, when the functions have steep fronts or sharp gradients the rational RBF method approximate them better than the standard RBF method [28]. These are the main reasons that we use rational RBF interpolants.

The RRBF interpolant of function $\mathbf{f}$ is given by

$$\mathcal{Q}(\boldsymbol{x}) = \frac{u(\boldsymbol{x})}{v(\boldsymbol{x})},$$

where satisfies in the interpolation conditions

$$\mathcal{Q}(\boldsymbol{x}_k^c) = \mathbf{f}(\boldsymbol{x}_k^c), \qquad k = 1, 2, ..., N$$

and $u(\boldsymbol{x})$ and $v(\boldsymbol{x})$ are the RBF interpolants

$$u(\boldsymbol{x}) = \sum_{j=1}^{N} c_j^u\ \psi\left(\|\boldsymbol{x} - \boldsymbol{x}_j^c\|_2\,,\,\epsilon\right)$$

and

$$v(\boldsymbol{x}) = \sum_{j=1}^{N} c_j^v\ \psi\left(\|\boldsymbol{x} - \boldsymbol{x}_j^c\|_2\,,\,\epsilon\right).$$

Let $\mathbf{u} = [u(\boldsymbol{x}_1^c), ..., u(\boldsymbol{x}_N^c)]^T$ and $\mathbf{v} = [v(\boldsymbol{x}_1^c), ..., v(\boldsymbol{x}_N^c)]^T$.

By applying the interpolation conditions we have a system of equations that is underdetermined, thus in order for the rational interpolant to be uniquely defined, we add an additional condition (for more descriptions see [16, 28]), which leads the native space semi-norms [10] of the RBF interpolants $u(\boldsymbol{x})$ and $v(\boldsymbol{x})$ to be minimized. By adding the condition we will have a minimization problem with the solution $\mathbf{v}$ which is the eigenvector corresponding to the smallest eigenvalue problem

$$R\mathbf{v} = \lambda\mathbf{v},$$

where

$$R = \operatorname{diag}\left(1/\left(\frac{\mathbf{f}^{\,2}}{\|\mathbf{f}\|_2^2} + 1\right)\right)\left(\frac{DA^{-1}D}{\|\mathbf{f}\|_2^2} + A^{-1}\right), \tag{2.4}$$

and in (2.4) A is the RBF system matrix given in (2.2), $\mathbf{f} = [f(\boldsymbol{x}_1^c), ..., f(\boldsymbol{x}_N^c)]^T$, $\|\mathbf{f}\|_2^2 = \sum_{j=1}^N f_j^{\,2}$ and $D = \operatorname{diag}(f(\boldsymbol{x}_1^c), ..., f(\boldsymbol{x}_N^c))$. Moreover, division is elementwise and $\mathbf{f}^{\,2}$ is an elementwise squaring of the elements of $\mathbf{f}$. When $\mathbf{v}$ is found, then $\mathbf{u}$ is obtained by $\mathbf{u} = D\mathbf{v}$. When $\mathbf{u}$ and $\mathbf{v}$ are found, we obtain the coefficients of the RBF interpolants by solving two linear systems,

$$Ac^u = \mathbf{u}, \quad \text{and} \quad Ac^v = \mathbf{v}. \tag{2.5}$$

Now we evaluate the rational interpolant at M points $\boldsymbol{x}_i$ by

$$\mathbf{Q} = \frac{Ec^u}{Ec^v}, \tag{2.6}$$

where division is elementwise, E is the RBF evaluation matrix (2.3) and $\mathbf{Q} = [\mathcal{Q}(\boldsymbol{x}_1), ..., \mathcal{Q}(\boldsymbol{x}_M)]^T$.

Now, we calculate the derivatives of the rational interpolant at N points $\boldsymbol{x}_k^c$ by applying quotient rule as below

$$\mathbf{Q}_1^{'} = \frac{(Ac^v).(E_Dc^u) - (Ac^u).(E_Dc^v)}{(Ac^v)^2}, \tag{2.7}$$

$$\mathbf{Q}_1^{''} = \frac{2(Ac^u).(E_Dc^v)^2 + (Ac^v)^2.(E_{DD}c^u) - (Ac^v).\Big(2\,(E_Dc^u).(E_Dc^v) + (Ac^u).(E_{DD}c^v)\Big)}{(Ac^v)^3}, \tag{2.8}$$

$$\mathbf{Q}_1^{'''} = \frac{I}{J}, \tag{2.9}$$

which

$$\begin{aligned} I = \Bigg(& 2(E_Dc^u).(E_Dc^v)^2 + 4(Ac^u).(E_Dc^v).(E_{DD}c^v) + 2(Ac^v).(E_Dc^v).(E_{DD}c^u) + (Ac^v)^2.(E_{DDD}c^u) \\ & -(E_Dc^v)\Big(2(E_Dc^u).(E_Dc^v) + (Ac^u).(E_{DD}c^v)\Big) - (Ac^v)\Big(2(E_{DD}c^u).(E_Dc^v) + 2(E_Dc^u).(E_{DD}c^v) \\ & +(E_Dc^u).(E_{DD}c^v) + (Ac^u).(E_{DDD}c^v)\Big)\Bigg).(Ac^v)^3 - 3(E_Dc^v).(Ac^v)^2.\Bigg(2(Ac^u).(E_Dc^v)^2 \\ & +(Ac^v)^2.(E_{DD}c^u) - (Ac^v).\Big(2(E_Dc^u).(E_Dc^v) + (Ac^u).(E_{DD}c^v)\Big)\Bigg), \end{aligned}$$

and

$$J = (Ac^v)^6,$$

where $\mathbf{Q}_1^{'} = \Big[\mathcal{Q}^{'}(\boldsymbol{x}_1^c), ..., \mathcal{Q}^{'}(\boldsymbol{x}_N^c)\Big]^T$, $\mathbf{Q}_1^{''} = \Big[\mathcal{Q}^{''}(\boldsymbol{x}_1^c), ..., \mathcal{Q}^{''}(\boldsymbol{x}_N^c)\Big]^T$, $\mathbf{Q}_1^{'''} = \Big[\mathcal{Q}^{'''}(\boldsymbol{x}_1^c), ..., \mathcal{Q}^{'''}(\boldsymbol{x}_N^c)\Big]^T$, A is the RBF system matrix, and E_D, E_{DD} and E_{DDD} are the first, second and third derivatives of evaluation matrix at N points $\boldsymbol{x}_k^c$.

It is concluded From equations (2.5) and (2.6) that the RRBF interpolant is made by the RBF interpolation matrix A. Therefor, we are able to provide error bounds for RRBF interpolation [8]. For this purpose we must consider $\mathbf{u}$ and $\mathbf{v}$ as the values obtained by sampling some functions r and $s \in \mathcal{N}_\psi(\Gamma)$ respectively.

Proposition 2.2. *Suppose $\Gamma \subseteq \mathbb{R}^{\mathrm{m}}$, $\psi \in C(\Gamma\times\Gamma)$ be a strictly positive definite RBF, and let that $X = \{\boldsymbol{x}_1^c, \boldsymbol{x}_2^c, ..., \boldsymbol{x}_N^c\} \subseteq \Gamma$ is a set of distinct points and $\mathcal{Q}$ is the RRBF interpolant to $f \in \mathcal{N}_\psi(\Gamma)$. Moreover, let us suppose that r and $s \in \mathcal{N}_\psi(\Gamma)$, Then for all $\boldsymbol{x} \in \Gamma$ we have*

$$|f(\boldsymbol{x}) - \mathcal{Q}(\boldsymbol{x})| \leq \frac{1}{|v(\boldsymbol{x})|}\left(|f(\boldsymbol{x})|\|s\|_{\mathcal{N}_\psi(\Gamma)} + \|r\|_{\mathcal{N}_\psi(\Gamma)}\right) P_{\psi,X}(\boldsymbol{x}).$$

So proposition 2.2 gives the error bound for the RRBF interpolant in terms of data values and power function, as for the standard RBF interpolant.

3. RRBFs method for solving KdV equation

Now, we use the RRBFs method to find the numerical solution of the KdV equation. In fact, we develop RRBFs to study the KdV equation with Dirichlet boundary conditions. In our method, we employ the derivatives of the RRBFs to approximate the spatial derivatives and then we apply an explicit, fourth-order Runge-Kutta (RK4) method to advance the resulting semi-discrete system in time.

In fact, we first approximate the spatial derivatives at N centers $\boldsymbol{x}_i^c$ at time t^n, i.e.

$$\mathbf{W}_x\left(x,t^n\right)=\left[W_x\left(\boldsymbol{x}_1^c,t^n\right),W_x\left(\boldsymbol{x}_2^c,t^n\right),...,W_x\left(\boldsymbol{x}_N^c,t^n\right)\right]^T,$$

and

$$\mathbf{W}_{xxx}\left(x,t^n\right)=\left[W_{xxx}\left(\boldsymbol{x}_1^c,t^n\right),W_{xxx}\left(\boldsymbol{x}_2^c,t^n\right),...,W_{xxx}\left(\boldsymbol{x}_N^c,t^n\right)\right]^T,$$

of the KdV equation (1.1) by RRBFs method, when

$$\mathbf{W}^n=\left[W\left(\boldsymbol{x}_1^c,t^n\right),W\left(\boldsymbol{x}_2^c,t^n\right),...,W\left(\boldsymbol{x}_N^c,t^n\right)\right]^T,$$

is considered instead of $\mathbf{f}$. This leads to a system of ordinary differential equations of the form

$$\mathbf{W}_t=G(\mathbf{W},t).$$

Then we apply RK4 method to solve the above equation as follows

$$\begin{aligned}
&\mathbf{K}_1=\Delta tG(\mathbf{W}^n,t^n),\\
&\mathbf{K}_2=\Delta tG(\mathbf{W}^n+0.5k_1,t^n+0.5\Delta t),\\
&\mathbf{K}_3=\Delta tG(\mathbf{W}^n+0.5k_2,t^n+0.5\Delta t),\\
&\mathbf{K}_4=\Delta tG(\mathbf{W}^n+k_3,t^n+\Delta t),\\
&\mathbf{W}^{n+1}=\mathbf{W}^n+\tfrac{1}{6}(\mathbf{K}_1+2\mathbf{K}_2+2\mathbf{K}_3+\mathbf{K}_4),
\end{aligned}\tag{3.1}$$

where $t^n=t^{n-1}+\Delta t$ and Δt is the time step size. Clearly, to obtain $\mathbf{W}^1$ initial value $\mathbf{W}^0$ is required in the iterative computation. Using the initial condition in (1.2), we have $\mathbf{W}^0=\left[g(\boldsymbol{x}_1^c),g(\boldsymbol{x}_2^c)\cdots,g(\boldsymbol{x}_N^c)\right]^T$.

To apply the Dirichlet boundary conditions (1.3), we directly replace $W\left(\boldsymbol{x}_1^c,t^n\right)$ with $w(a,t^n)=h(t^n)$ and $W\left(\boldsymbol{x}_N^c,t^n\right)$ with $w(b,t^n)=l(t^n)$.

4. Stability issue

Since the RRBFs interpolant is constructed by using the standard RBFs interpolation matrix, the RRBFs method can also suffer of instability problems, especially for $\epsilon\to 0$. In fact, serious problems of ill-conditioning may occur by choosing wrong values of the shape parameter, particularly for infinitely smooth RBFs. In order for the system matrix A to be well-conditioned, the shape parameter ϵ must not be too small, but small shape parameters are required to obtain better accuracy for the interpolation with RBFs. This is known as the Uncertainty Principle. We choose the shape parameter ϵ so that the collocation matrix A has a $O(10^{16})$ condition number, in order to determine the proper value for ϵ [28]. These values for the condition number are valid when using a computer that implements double precision floating point arithmetic, but the bounds will be different when using other floating point number systems.

5. Numerical results

In this section, we consider five examples of the KdV equation to validate the presented method and assess the efficiency and accuracy of the method by calculating L_∞, L_2 and RMS error norms. Also, we compare the results with other methods.

L_∞, L_2 and RMS error norms are given by the following formulas:

$$L_\infty = \|\mathbf{W} - \mathbf{w}\|_\infty,$$
$$L_2 = \|\mathbf{W} - \mathbf{w}\|_2,$$
$$RMS = \sqrt{\frac{1}{N}\|\mathbf{W} - \mathbf{w}\|_2}.$$

where $\mathbf{W}$, $\mathbf{w}$ are the approximate and the exact solutions respectively.

Since the solution of the KdV equation satisfies in many conservation laws, we will investigate three conservation quantities of the KdV equation, i.e., mass, momentum and energy, which are defined in [14] as below,

$$E_1 = \int_a^b w(x)^n dx,$$
$$E_2 = \int_a^b \left(w\left(x\right)^n\right)^2 dx,$$
$$E_3 = \int_a^b \left[\left(w\left(x\right)^n\right)^3 - \frac{3\mu}{\varepsilon}\left(w_x^n\left(x\right)\right)^2\right] dx.$$

Also for calculating the above integrals we will use the composite trapezoidal rule for integration. Moreover, in all numerical examples we have used uniformly spaced centers

$$x_i^c = a + \frac{i-1}{N-1}(b-a), \qquad i = 1, 2, \cdots N, \tag{5.1}$$

or non-uniformly spaced centers

$$x_i^c = \frac{1}{2}\left(-(b-a)\left(\frac{\arcsin\left(0.999\cos(\pi(i-1)/(N-1))\right)}{\arcsin(0.999)}\right) + (b+a)\right), \quad i = 1, 2, ..., N, \tag{5.2}$$

which are clustered mildly around the boundaries [28].

We calculate the rate of convergence in space and time respectively, by using the following formulas

$$O_{c_s} = \frac{\log_{10}\left(\frac{e_{N_i}}{e_{N_{i+1}}}\right)}{\log_{10}\left(\frac{N_{i+1}}{N_i}\right)} \qquad \text{and} \qquad O_{c_t} = \frac{\log_{10}\left(\frac{e_{(\Delta t)_i}}{e_{(\Delta t)_{i+1}}}\right)}{\log_{10}\left(\frac{(\Delta t)_i}{(\Delta t)_{i+1}}\right)},$$

where e_{N_i} indicates the error of the method with N_i points and $e_{(\Delta t)_i}$ indicates the error of the method with time step size $(\Delta t)_i$.

For rational interpolation the selection of the shape parameter ϵ is a tedious computational issue. Indeed, wrong choices of the shape parameter might lead to serious problems of ill-conditioning, especially for infinitely smooth RBFs. Therefore, the choice of the shape parameter is crucial and can be selected such that it is optimal. The shape parameter for all the calculations performed in this paper was found experimentally. In fact, in all examples, the shape parameter was selected so that the condition number of the system matrix A with elements given in Eq. (5) has a $O(10^{16})$ condition number. The shape parameter selected in this way results the most accurate approximations. Numerical computations have been done with Matlab on Intel(R) Core(TM) i3 CPU 2.53 GHz and 4 GB of RAM.

Example 5.1. Consider the KdV equation (1.1) with $\mu = 4.84 \times 10^{-4}, \varepsilon = 1$, and analytical solution as follows [3, 7, 19]

$$w(x,t) = 3h\,\mathrm{sech}^2(D + Bx - Ct), \quad 0 \le x \le 2,$$

where

$$B = \frac{1}{2}\sqrt{\frac{\varepsilon h}{\mu}}, \quad C = \varepsilon r B, \quad D = -6, \text{ and } h = 0.3.$$

TABLE 1. Conservation quantities, errors and CPU time of the Example 5.1.

	RRBF (Inverse quadratic)						[7]
t	L_∞	L_2	E_1	E_2	E_3	$CPU\ time\ (s)$	$CPU\ time$
0	0	0	0.144598	0.086759	0.047747	-	-
0.25	2.6575e-03	6.1898e-03	0.144382	0.086760	0.047747	10	-
0.5	3.9688e-03	9.6891e-03	0.144227	0.086761	0.047747	19	35
1	5.3453e-03	1.4910e-02	0.143920	0.086764	0.047743	40	63
1.5	6.3183e-03	2.0028e-02	0.143743	0.086766	0.047747	52	88
2	7.7015e-03	2.3193e-02	0.143540	0.086769	0.047731	70	115

We obtain the initial and Dirichlet boundary conditions from the analytical solution, and solve this problem with the RRBFs method by using the IQ and GA RBFs with $k = \Delta t = 0.001$, $N = 100$ uniformly spaced centers and the shape parameter $\epsilon = 8$ and $\epsilon = 27$, respectively. The exact values of the three invariants are $E_1 = 0.144598$, $E_2 = 0.086759$, $E_3 = 0.047747$. We show the L_∞, L_2, RMS errors, the numerical values of E_1, E_2 and E_3 and CPU time at different times in Table 1 and Table 2. As can be seen in these tables the values of the invariants remain almost constant, the better accuracy is obtained compared with [7] and [19] and GA function gives a better approximation compared to IQ, although CPU time increases. In Table 3 (left) the number of points is kept fixed at $N = 100$ and the time step size is varied to compute the time rate of convergence for IQ RBF with $\epsilon = 8$, also in this table (right) the time step size is kept fixed at $\Delta t = 0.0001$ and number of points is varied to compute the space rate of convergence for GA RBF with $\epsilon = 27$ at time $t = 1$. Figure 1 shows the exact and numerical solution s at time $t = 1$ for the case of the IQ RBF. It can be seen that they are well matched with each other. We also show the space-time graph of the estimated solution in Figure 1.

TABLE 2. Errors and CPU time of the Example 5.1.

	RRBF (Gaussian)				[7]	[19]
t	L_∞	L_2	RMS	$CPU\ time\ (s)$	L_∞	L_∞
0	0	0	0	-	-	-
0.1	6.4213e-04	1.1778e-03	1.1778e-04	15	-	2.1500e-02
0.25	5.8580e-04	1.9348e-03	1.9348e-04	32	-	-
0.5	5.9262e-04	2.9307e-03	2.9307e-04	64	7.2329e-04	-
1	6.8047e-04	3.6704e-03	3.6704e-04	125	1.7957e-03	-
1.5	7.5295e-03	2.5556e-02	2.5556e-03	190	3.8906e-03	-

Example 5.2. Now, we study the KdV equation (1.1) with $\mu = 1$ and $\varepsilon = 6$. The exact solution is given in [3, 7] as

$$w(x,t) = 12\left[\frac{\cosh(4x-64t)+4\cosh(2x-8t)+3}{(\cosh(3x-36t)+3\cosh(x-28t))^2}\right], \quad -5 \le x \le 15.$$

The boundary and initial conditions are extracted from the exact solution. We solve this example with the RRBFs method using IQ RBF, $k = \Delta t = 0.001$, shape parameter $\epsilon = 1.85$, and $N = 101$ centers according to (5.2).

The graph of exact and numerical solutions at time $t = 0.2$ and space-time graph of the numerical solution are shown in Figure 2. In Table 4, we compute the L_∞, L_2, RMS errors and CPU time at different times (during the

TABLE 3. Convergence rates in time and space of the Example 5.1.

	Convergence rate in time				Convergence rate in space		
	Δt	L_2	O_{c_t}		N	L_∞	O_{c_s}
$\epsilon = 8$	1.0000e-03	1.4910e-02	-	$\epsilon = 27$	32	3.5974e-01	-
	5.0000e-04	1.5312e-02	-0.038398		64	2.1668e-02	4.053
	2.5000e-04	1.5013e-02	0.028468		128	2.5765e-04	6.394
	1.2500e-04	1.4910e-02	0.009929		256	2.5783e-04	-0.001
	6.2500e-05	1.4917e-02	0.009252		512	1.5134e-04	0.678
	3.1250e-05	1.4910e-02	0.000675				

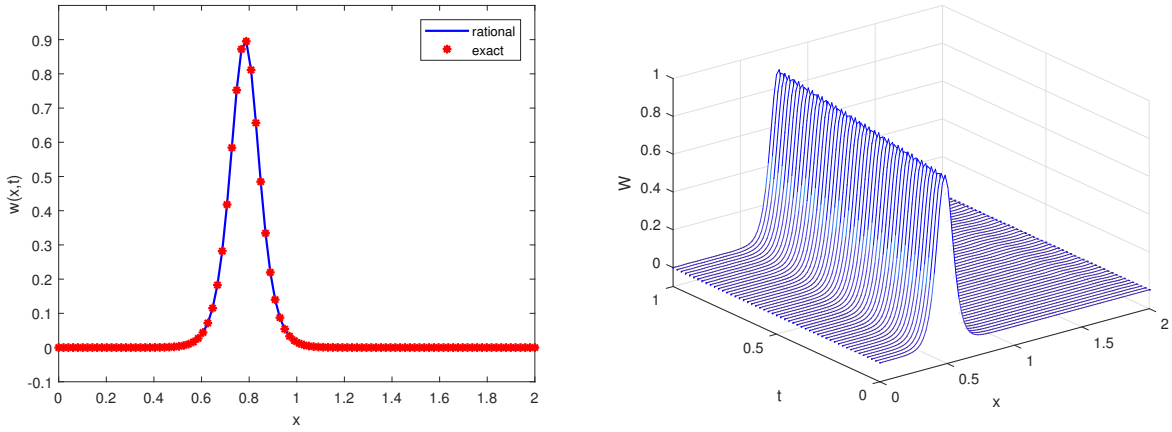

(A) RRBF and exact solutions at time t=1. (B) space-time graph.

FIGURE 1. Numerical results for the solution of Example 5.1.

interaction and after the interaction). It can be seen from Table 4 that the results of the method are well matched with [7] and the CPU time is reduced.

TABLE 4. Errors and CPU time of the Example 5.2.

	RRBF				[7]	
t	L_∞	L_2	RMS	$CPU\ time\ (s)$	L_∞	$CPU\ time$
0.001	1.2161e-03	2.6330e-03	2.6199e-04	0.9	-	-
0.005	1.6887e-03	4.8792e-03	4.8550e-04	1.2	-	-
0.01	2.3159e-03	6.0763e-03	6.0461e-04	1.5	-	-
0.05	2.4739e-02	4.4692e-02	4.4470e-03	5	-	-
0.1	3.6000e-02	7.7000e-02	7.7000e-03	8	5.6355e-03	59
0.2	4.5598e-02	1.3911e-01	1.3842e-02	12.4	2.3376e-02	110
0.3	7.0813e-02	2.1408e-01	2.1301e-02	18.5	5.9437e-02	161

Example 5.3. In this example, we examine the KdV equation (1.1) with $\mu = 4.84 \times 10^{-4}, \varepsilon = 1$ and with the analytical solution [3, 14, 19]

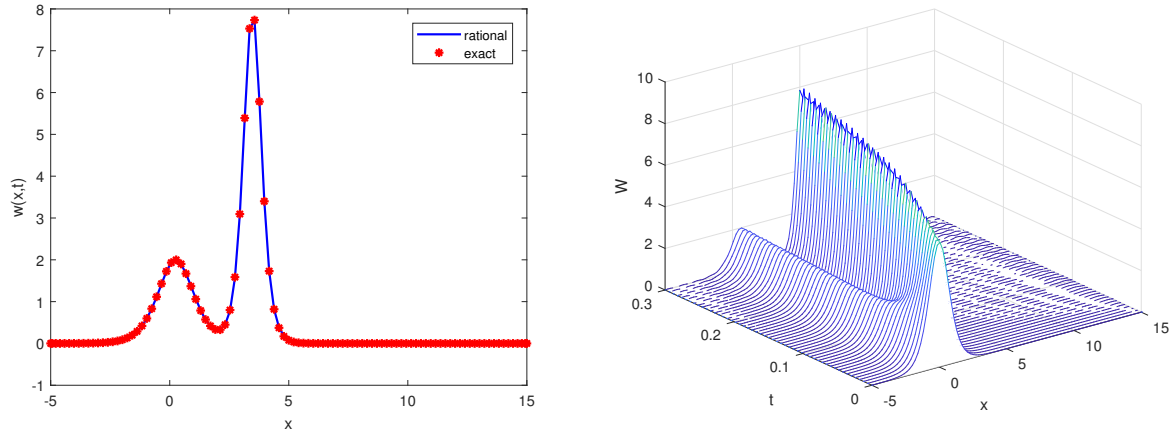

(A) RRBF and exact solutions at time $t = 0.2$.

(B) space-time graph.

FIGURE 2. Numerical results for the solution of Example 5.2.

$$w(x,t) = 12\mu(\log F)_{xx}, \quad 0 \le x \le 4,$$

where

$$F = 1 + e^{\eta_1} + e^{\eta_2} + \left(\frac{\alpha_1 - \alpha_2}{\alpha_1 + \alpha_2}\right)^2 e^{\eta_1+\eta_2},$$
$$\eta_i = \alpha_i x - \alpha_i^3 \mu t + b_i, \quad i = 1, 2,$$
$$\alpha_1 = \sqrt{\frac{0.3}{\mu}}, \quad \alpha_2 = \sqrt{\frac{0.1}{\mu}}, \quad b_1 = -0.48\alpha_1, \quad b_2 = -1.07\alpha_2.$$

The initial and Dirichlet boundary conditions are derived from the analytical solution. We use $N = 100$ uniformly spaced centers, shape parameter $\epsilon = 8$ and $N = 200$ uniformly spaced centers, shape parameter $\epsilon = 33$ when using the IQ and GA RBF, respectively. The analytical values of the three conservation quantities are $E_1 = 0.228081$, $E_2 = 0.103456$, $E_3 = 0.049855$. We show the L_∞, L_2, RMS errors, CPU time and the approximate values of E_1, E_2 and E_3 at several times with $k = \Delta t = 0.01$ and $k = \Delta t = 0.001$ in Table 5 and Table 6, respectively. As shown in the tables the values of the Conservation quantities remain nearly constant and the better accuracy is obtained compared with [14] and [19].

Figure 3 shows the exact and approximate solution s at time $t = 1$ for the case of the IQ RBF. It can be seen that they are well matched with each other. Also, the numerical solution is simulated for $t = 0.1$ in Figure 3.

Example 5.4. In this example, the interaction of two solitary waves to the KdV equation (1.1) with $\mu = 1$ and $\varepsilon = 6$ is studied. The exact solution is given in [3, 7] as

$$w(x,t) = 5\left[\frac{2\text{sech}^2(x - 4t + 12) + 4.5\text{csch}^2 1.5(x - 9t + 14.5)}{(-2\tanh(x - 4t + 12) + 3\coth 1.5(x - 9t + 14.5))^2}\right],$$

in the region $-20 \le x \le 0$, we obtain the initial and Dirichlet boundary conditions from the analytical solution and solve this problem with the RRBFs method by using the IQ RBF with $k = \Delta t = 0.001$, $N = 100$ uniformly and

TABLE 5. Conservation quantities, errors and CPU time of the Example 5.3.

	RRBF (IQ)						
t	L_∞	L_2	RMS	E_1	E_2	E_3	$CPU\ time$
0	0	0	0	0.228081	0.103456	0.049855	-
0.005	1.3210e-04	2.7703e-04	2.7703e-05	0.228082	0.103456	0.053086	0.6
0.01	2.8430e-04	5.4033e-04	5.4033e-05	0.228082	0.103455	0.053086	0.7
0.25	4.8000e-03	5.9000e-03	5.9424e-04	0.227897	0.103435	0.053064	2.5
1	4.0000e-03	1.4000e-02	1.4000e-03	0.227650	0.103374	0.052995	5
2	7.0000e-03	2.0800e-02	2.0000e-03	0.227429	0.103325	0.052670	9
3	1.0009e-02	3.5139e-02	3.5139e-03	0.226775	0.103307	0.050029	17

TABLE 6. Conservation quantities and errors of the Example 5.3.

	RRBF (GA)					[14]	[19]
t	L_∞	L_2	E_1	E_2	E_3	L_∞	L_∞
0	0	0	0.228081	0.103456	0.050764	0	0
0.005	7.7333e-07	1.4430e-06	0.228081	0.103456	0.050764	7.30e-03	6.90e-03
0.01	1.0938e-06	1.8410e-06	0.228081	0.103456	0.050764	1.49e-02	1.41e-02
0.25	1.3142e-05	4.4070e-05	0.228082	0.103456	0.050763	-	-
1	1.7189e-05	1.0142e-04	0.228083	0.103456	0.050759	-	-
2	2.4871e-03	6.6633e-03	0.228082	0.103456	0.050668	-	-
3	1.3285e-03	3.8389e-03	0.228083	0.103456	0.049951	-	-
10	2.7227e-03	7.3189e-03	0.228080	0.103456	0.050764	-	-

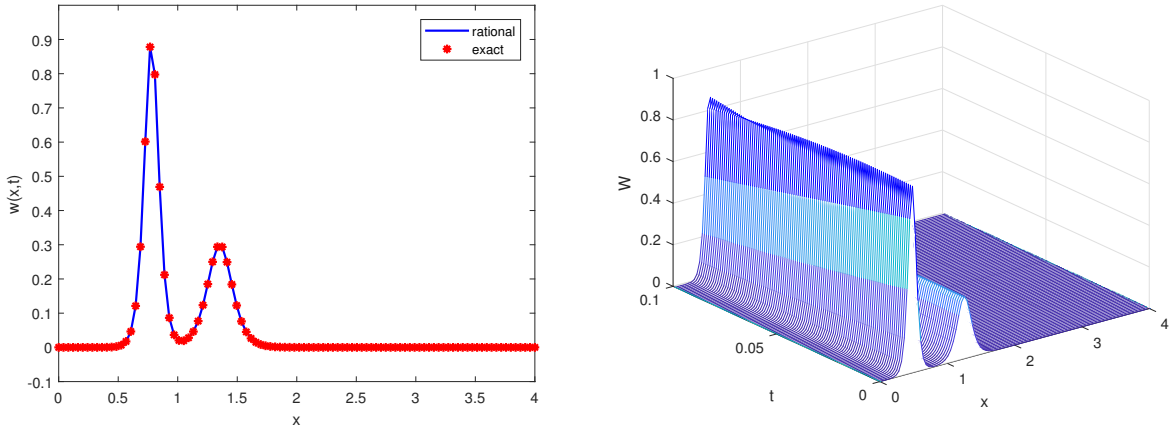

(A) RRBF and exact solutions at time $t = 1$.

(B) space-time graph.

FIGURE 3. Numerical results for the solution of Example 5.3.

non-uniformly spaced centers given by (5.1) and (5.2) and the shape parameter $\epsilon = 1.7$. Graph of the approximate and exact solution s at time $t = 1$ and space-time graph of the numerical solution are shown in Figure 4. Table 7

shows the L_∞, L_2, RMS errors and CPU time at several times. From Table 7, it can be seen that the RRBFs method solves the problem accurately, also the results of the method are well matched with analytical solutions and the earlier works, and compared to [7] cpu time is reduced. Also, the comparison of numerical results show that the adoption of non-uniform nodes provides improved numerical results. In Table 8 (left) the number of uniform points is kept fixed at $N = 100$ and the time step size is varied to compute the time rate of convergence with $\epsilon = 1.7$, also in this table (right) the time step size is kept fixed at $\Delta t = 0.00001$ and number of points is varied to compute the space rate of convergence for IQ RBF with $\epsilon = 2.2$ at time $t = 0.1$.

TABLE 7. Errors and CPU time of the Example 5.4.

	RRBF (Non-uniform points (5.2))		RRBF (Uniform points (5.1))			[7]
t	L_∞	L_2	L_∞	L_2	$CPU\ time$	$CPU\ time$
0.005	1.9228e-03	3.2914e-03	2.4659e-03	3.0244e-03	-	-
0.01	2.6272e-03	4.7409e-03	3.4726e-03	5.2751e-03	-	-
0.05	2.0525e-02	3.9505e-02	3.5171e-02	6.4529e-02	-	-
0.1	2.9989e-02	6.6307e-02	5.0277e-02	1.01581e-01	7	21
0.3	4.9577e-02	1.2834e-01	6.9620e-02	1.9110e-01	18	63
0.5	5.9081e-02	1.7279e-01	8.7088e-02	2.5214e-01	28	101
0.7	7.1093e-02	2.1654e-01	1.0214e-01	3.1508e-01	39	145
1	9.2518e-02	2.9707e-01	1.3610e-01	4.3173e-01	49	206

TABLE 8. Convergence rates in time and space of the Example 5.4.

	Convergence rate in time				Convergence rate in space		
	Δt	L_∞	O_{c_t}		N	L_∞	O_{c_s}
$\epsilon = 1.7$	1.0000e-03	0.050277	-	$\epsilon = 2.2$	40	5.4842e-01	-
	5.0000e-04	0.050636	-0.010282		80	6.3879e-02	3.1018
	2.5000e-04	0.051086	-0.012754		160	1.2259e-02	2.3814
	1.2500e-04	0.051108	-0.000631		320	1.1450e-02	0.0985
	6.2500e-05	0.051097	0.000321		640	1.0233e-02	0.1621
	3.1250e-05	0.051104	-0.000211				

Example 5.5. Consider the interactions of four solitons to the KdV equation (1.1) with $\varepsilon = 1$ and $\mu = 1$. In this case the initial and boundary conditions are derived from the analytical solution [14, 19]

$$w(x,t) = \sum_{i=1}^{4} 12\lambda_i^2 \mathrm{sech}^2(\lambda_i(-x_i - 4\lambda_i^2 t + x)), \quad -150 \le x \le 150,$$

where

$$\lambda_1 = 0.3,\ \lambda_2 = 0.25,\ \lambda_3 = 0.2,\ \lambda_4 = 0.15,$$
$$x_1 = -85,\ x_2 = -60,\ x_3 = -35,\ x_4 = -10.$$

We solve this problem with the RRBFs method by using the IQ RBF with $k = \Delta t = 0.001$, $N = 200$ uniformly spaced centers, the shape parameter $\epsilon = 0.09$ and $\epsilon = 0.3$. Graph of the approximate and exact solution s at time

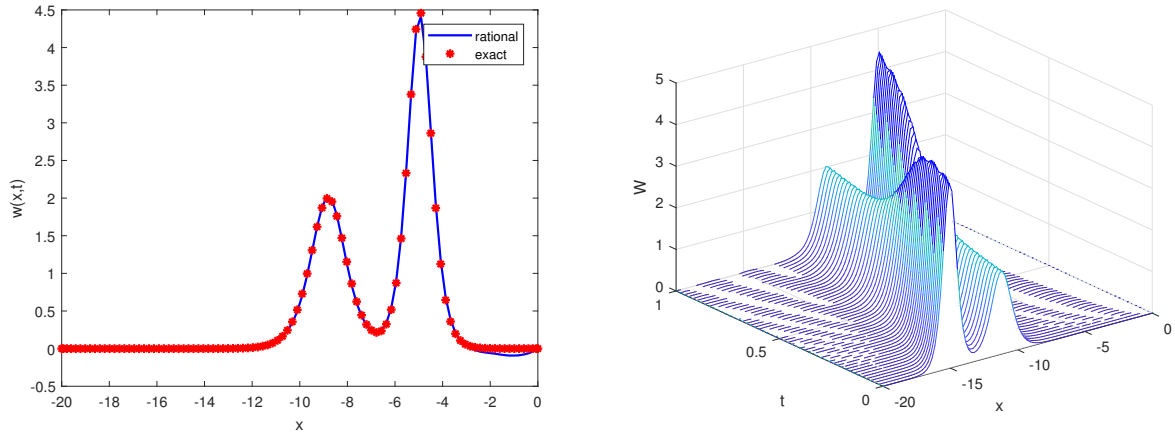

(A) RRBF and exact solutions at time $t = 1$.

(B) space-time graph.

FIGURE 4. Numerical results for the solution of Example 5.4.

$t = 2$ and space-time graph of the numerical solution are shown in Figure 5. The exact values of the three conservation quantities are $E_1 = 21.6000$, $E_2 = 10.3887$, $E_3 = 5.5266$. Table 9 shows the L_∞, L_2, RMS errors and the numerical values of E_1, E_2 and E_3 at different times up to $t = 100$. As can be seen in this table the values of the invariants are almost constant. The RRBFs method is able to solve the problem accurately, also the results obtained from this method are well matched with analytical solutions. In Table 10 (left) the number of points is kept fixed at $N = 200$ and the time step size is varied to compute the time rate of convergence with $\epsilon = 0.09$, also in this table (right) the time step size is kept fixed at $\Delta t = 0.001$ and number of points is varied to compute the space rate of convergence for IQ RBF with $\epsilon = 0.4$ at time $t = 2$.

TABLE 9. Conservation quantities and errors of the Example 5.5.

		RRBF					
t		L_∞	L_2	RMS	E_1	E_2	E_3
0	$\epsilon = 0.09$	0	0	0	21.6000	10.3887	5.5266
0.25		7.3398e-05	1.3232e-04	9.3568e-06	21.6000	10.3887	5.5266
0.5		1.7461e-04	3.0252e-04	2.1391e-05	21.6000	10.3887	5.5267
1		2.4064e-04	4.1193e-04	2.9128e-05	21.6000	10.3888	5.5267
1.5		2.6193e-04	4.7765e-04	3.3775e-05	21.6000	10.3888	5.5267
2		1.8298e-04	5.6079e-04	3.9654e-05	21.5999	10.3888	5.5267
3		6.7408e-04	9.8966e-04	6.9979e-05	21.5992	10.3888	5.5267
10	$\epsilon = 0.3$	9.7801e-03	1.8276e-02	1.2923e-03	21.5974	10.3840	5.5272
20		2.3187e-02	5.0943e-02	3.6022e-03	21.5810	10.3818	5.5219
50		3.2589e-02	1.4680e-01	1.0380e-02	21.6489	10.4255	5.5096
100		5.7655e-02	2.2401e-01	1.5840e-02	21.6249	10.4689	5.4658

TABLE 10. Convergence rates in time and space of the Example 5.5.

	Convergence rate in time				Convergence rate in space		
	Δt	L_∞	O_{c_t}		N	L_∞	O_{c_s}
$\epsilon = 0.09$	5.0000e-01	1.7755e-04	-	$\epsilon = 0.4$	50	1.3265e-01	-
	2.5000e-01	1.8788e-04	-0.0979611		100	1.2986e-01	0.03
	1.2500e-01	1.9543e-04	-0.0568423		200	2.7290e-02	2.25
	6.2500e-02	1.9591e-04	-0.0035398		400	5.3723e-04	5.66
	3.1250e-02	1.9594e-04	-0.0001926		800	2.9900e-03	-2.47
	1.5625e-02	1.9594e-04	-0.0000108				
	7.8125e-03	1.9594e-04	-0.0000006				

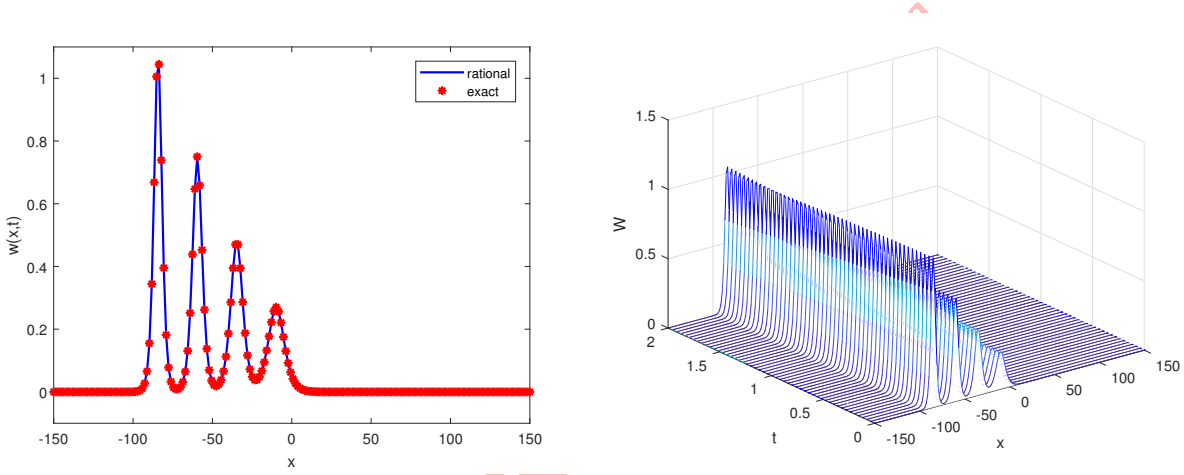

(A) RRBF and exact solutions at time $t = 2$.

(B) space-time graph.

FIGURE 5. Numerical results for the solution of Example 5.5.

6. CONCLUSION

This paper investigates the application of the RRBFs method to find the numerical solution of the KdV equation with Dirichlets's boundary conditions, especially when the equation has a solution with steep front or sharp gradients. The combination of RRBFs in space and RK4 in time, gives accurate and reliable solutions to the KdV equation. To illustrate the accuracy and efficiency of the presented method, we carried out five examples and presented the corresponding graphs and tables. In addition, for some examples, the conservation laws is investigated. As reported by numerical examples, it can be said that the presented scheme provides accurate numerical solutions and is useful for simulating the motions, interactions and conservation properties of solitary waves for the KdV equation.

REFERENCES

[1] E.N. Aksan, A. Özdes, *Numerical solution of Korteweg–de Vries equation by Galerkin B-spline finite element method*, Appl. Math. Comput. *175* (2006) 1256-1265.

[2] A. Bashan, *An effective application of differential quadrature method based on modified cubic B-splines to numerical solutions of the KdV equation*, Turk. J. Math. *42* (2018) 373-394.

[3] A. Bashan, A. Esen, *Single soliton and double soliton solutions of the quadratic-nonlinear Korteweg-de Vries equation for small and long-times*, Numer. Methods Partial Differential Equations (2020) 1-22.

[4] R.C. Cascaval , *Variable coefficient KdV equations and waves in elastic tubes*, Lect. Notes Pure Appl. Math. *234* (2003) 57-70.

[5] D.G. Crighton , *Applications of KdV*, Acta Appl. Math. *39* (1995) 39-67.

[6] I. Dağ, Y. Dereli, *Numerical solutions of KdV equation using radial basis functions*, Appl. Math. Model. *32* (2008) 535-546.

[7] M. Dehghan, A. Shokri, *A numerical method for KdV equation using collocation and radial basis functions*, Nonlinear Dyn. *50* (2007) 111-120.

[8] S. De Marchi, A. Martinez, E. Perracchione, *Fast and stable rational RBF-based partition of unity interpolation*, J. Comput. Appl. Math. *349* (2019) 331-343.

[9] A. Durán, M.A. Lopez-Marcos, *Conservative numerical methods for solitary wave interactions*, J. Phys. A. *36* (2003) 7761-7770.

[10] G.E. Fasshauer. *Meshfree Approximation Methods with Matlab*, World Scientific, 2007.

[11] B. Fornberg, G.B. Whitham, *A numerical and theoretical study of certain nonlinear wave phenomena*, Philos. Trans. Roy. Soc. *289* (1978) 373-404.

[12] C.S. Gardner, G.K. Morikawa, *Similarity in the Asymptotic Behavior of Collision-free Hydromagnetic Waves and Water Waves*, New York Univ., Inst. of Mathematical Sciences, Technical Report, 1960.

[13] K. Goda, *On instability of some finite difference schemes for Korteweg-de Vries equation*, J. Phys. Soc. Japan *39* (1975) 229-236.

[14] S.Y. Hao, S.S. Xie, S.C. Yi, *The Galerkin method for the KdV equation using a new basis of smooth piecewise cubic polynomials*, Appl. Math. Comput. *218* (2012) 8659-8671.

[15] M. Heidari, M. Mohammadi, S. De Marchi, *A shape preserving quasi-interpolation operator based on a new transcendental RBF*, Dolomites Research Notes on Approximation *14* (1) (2021) 56-73.

[16] S. Jakobsson, B. Andersson, F. Edelvik, *Rational radial basis function interpolation with applications to antenna design*, J. Comput. Appl. Math. *233* (2009) 889-904.

[17] A. Jeffrey, T. Kakutani, *Weak nonlinear dispersive waves: a discussion centered around the Korteweg–de Vries equation*, SIAM Rev. *14* (4) (1972) 582-643.

[18] S.B.G. Karakoc, K.K. Ali, *New exact solutions and numerical approximations of the generalized KdV equation*, Comput. Methods Differ. Equ. *9* (3) (2021) 670-691.

[19] D. Kong, Y. Xu, Z. Zheng, *A hybrid numerical method for the KdV equation by finite difference and sinc collocation method*, Appl. Math. Comput. *355* (2019) 61-72.

[20] D.J. Korteweg, G. De Vries, *On the change of form of long waves advancing in a rectangular canal, and on a new type of long stationary waves*, Philos. Mag. *39* (240) (1895) 422-443.

[21] M. Lakestani, *Numerical solutions of the KdV equation using B-spline functions*, Iran. J. Sci. Technol. Trans. A Sci. *41* (2017) 409-417.

[22] M. Mohammadi, R. Mokhtari, R. Schaback, *A meshless method for solving the 2d brusselator reaction-diffusion system*, Comput. Model. Eng. Sci. *101*(2014)113–138.

[23] R. Najafi, *Approximate nonclassical symmetries for the time-fractional KdV equations with the small parameter*, Comput. Methods Differ. Equ. *8* (1) (2020) 111-118.

[24] S.L. Naqvi, J. Levesley, S. Ali, *Adaptive radial basis function for time dependent partial differential equations*, J. Prime Res. Math. *13* (2017) 90-106.

[25] S. Niknam, H. Adibi, *A numerical solution of two-dimensional hyperbolic telegraph equation based on moving least square meshless method and radial basis functions*, Comput. Methods Differ. Equ. *10* (4) (2022) 969-985.

[26] Ö. Oruç, F. Bulut, A. Esen, *Numerical solution of the KdV equation by Haar wavelet method*, Pramana-J. Phys. *87* (94) (2016) 1-11.

[27] B. Saka, *Cosine expansion-based differential quadrature method for numerical solution of the KdV equation*, Chaos Solitons Fractals *40* (2009) 2181-2190.

[28] S.A. Sarra, Y. Bai, *A rational radial basis function method for accuratly resolving discontinuities and steep gradients*, Appl. Numer. Math. *130* (2018) 131-142.
[29] R. Schaback, *Kernel-Based Meshless Methods*, Gottingen, 2011.
[30] M. Shiralizadeh, A. Alipanah, M. Mohammadi, *Numerical solution of one-dimensional Sine-Gordon equation using rational radial basis functions*, J. Math. Model. *10* (2022) 1-16.
[31] L. Van Wijngaarden, *On the equations of motion for mixtures of liquid and gas bubbles*, J. Fluid Mech. *33* (3) (1968), 465-474.
[32] A.C. Vliengenthart, *On finite difference methods for the Korteweg–de Vries equation*, J. Eng. Math. *5* (1971) 137-155.
[33] H. Washimi, T. Taniuti, *Propagation of ion-acoustic solitary waves of small amplitude*, Phys. Rev. Lett. *17* (1966) 996-998.
[34] H. Wendland, *Scattered data approximation*, Cambridge University Press, 2004.
[35] N.J. Zabusky, *A Synergetic Approach to Problem of Nonlinear Dispersive Wave Propagation and Interaction*, in: W. Ames (Ed.), Proc. Symp. Nonlinear Partial Diff. Equations, Academic Press, (1967) 223-258.